0026-895X/08/7305-1568–1577$20.00
MOLECULAR PHARMACOLOGY
Copyright © 2008 The American Society for Pharmacology and Experimental Therapeutics
Mol Pharmacol 73:1568–1577, 2008

Vol. 73, No. 5
42010/3334570
Printed in U.S.A.

Targeting *MDR1* Gene: Synthesis and Cellular Study of Modified Daunomycin-Triplex-Forming Oligonucleotide Conjugates Able to Inhibit Gene Expression in Resistant Cell Lines[S]

Vérène Stierlé, Maria Duca, Ludovic Halby, Catherine Senamaud-Beaufort, Massimo L. Capobianco, Alain Laigle, Béatrice Jollès, and Paola B. Arimondo

Laboratoire de Biophysique Moléculaire, Cellulaire et Tissulaire, Centre National de la Recherche Scientifique, Unité Mixte de Recherche 7033, Université Pierre et Marie Curie-Paris 6, Paris, France (V.S., A.L., B.J.); Université Paris 13, Bobigny, France (V.S., A.L., B.J.); Laboratoire de Régulation et Dynamiques des Génomes Centre National de la Recherche Scientifique, Unité Mixte de Recherche 5153, Muséum national d'Histoire naturelle USM0503 (M.D., L.H., C.S.-B., P.B.A.); Institut National de la Santé et de la Recherche Médicale UR565, Paris cedex 05, France (M.D., L.H., C.S.-B., P.B.A.); and Istituto per la Sintesi Organica e la Fotoreattività del Consiglio Nazionale delle Ricerche, Bologna, Italy (M.L.C.)

Received September 20, 2007; accepted February 25, 2008

ABSTRACT

Reversal of the multidrug-resistant (MDR) phenotype is very important for chemotherapy success. In fact, the expression of the *MDR1* gene-encoded P-glycoprotein (P-gp) actively expels antitumor agents such as daunomycin (DNM) out of the cells, resulting in drug resistance. We show that upon conjugation to triplex-forming oligonucleotides, it is possible to address DNM in resistant cells (MCF7-R and NIH-MDR-G185). The oligonucleotide moiety of the conjugate changes the cellular penetration properties of the antitumor agent that is no more the target of P-gp in resistant cells. We observe an accumulation of conjugated DNM in cells up to 72 h. For more efficient delivery in the cells' nuclei, transfectant agents must be used. In addition, the conjugate recognizes a sequence located in exon 3 of *MDR1*, and it inhibits its gene expression as measured both by Western blot and by reverse transcription-polymerase chain reaction.

Conventional cancer chemotherapy is seriously limited by the multidrug resistance (MDR) commonly acquired by tumor cells (Pérez-Tomás, 2006). One mechanism by which a living cell can achieve multiple resistances is via the active efflux by MDR proteins of a broad range of anticancer drugs through the cellular membrane. *MDR1* (*ABCB1*) overexpression is one form of MDR; the gene encodes for the 170-kDa P-glycoprotein (P-gp), a transmembrane pump that causes efflux of organic compounds out of cells. Among drugs that commonly act as substrates of P-gp is, for example, the family of the anthracyclines such as daunomycin (DNM). A consistent amount of research has been devoted to MDR reversal. Many compounds able to modulate this phenotype in vitro by inhibiting the efflux pump activity of P-gp have been found. However, their clinical application is limited because of their high toxicity. Therefore, attention has been drawn to the selective down-regulation of *MDR1* expression through antisense (Quattrone et al., 1994; Bertram et al., 1995; Alahari et al., 1996; Liu et al., 1996), and, more recently, small interfering RNA (siRNA) (Nieth et al., 2003; Wu et al., 2003; Duan et al., 2004).

In addition to these approaches, the antigene strategy can also be used to specifically modulate gene expression. It is based on triplex-forming oligonucleotides (TFOs) that bind DNA and target specifically purine-rich sequences by forming a DNA triple helix. The high frequency of triplex target sequences in the genome, together with the high sequence

This work was supported by grants from the Ligue Nationale contre le Cancer, Ministère de la Recherche et de l'Industrie ACI "Molécules et Cibles Thérapeutiques" (to P.B.A.), Coopération Centre National de la Recherche Scientifique-Consiglio Nazionale delle Ricerche (to P.B.A. and to M.C.), and Association pour la Recherche contre le Cancer (ARC) (to M.D.).

V.S. and M.D. contributed equally to this work.

Article, publication date, and citation information can be found at http://molpharm.aspetjournals.org.
doi:10.1124/mol.107.042010.

[S] The online version of this article (available at http://molpharm.aspetjournals.org) contains supplemental material.

ABBREVIATIONS: MDR, multidrug resistance; P-gp, P-glycoprotein; DNM, daunomycin; siRNA, small interfering RNA; TFO, triplex-forming oligonucleotide; P, 5-propynyluracils; M, 5-methylcytosines; LNA, locked nucleic acid; HPLC, high-performance liquid chromatography; AS, antisense; MS, mass spectrometry; C_{50}, concentration at which 50% of triplex is formed; RT-PCR, reverse transcription-polymerase chain reaction; OFA, Oligofectamine; PBS, phosphate-buffered saline; bp, base pair(s); T_m, melting temperature; R, oligopurine strand of the duplex; Y, oligopyrimidine strand of the duplex.

specificity of TFOs, makes these molecules effective tools to modulate in a selective manner gene expression via transcriptional repression, mutagenesis, and recombination. In fact, triplex approaches have been applied with success in various experimental models, including living cells and animals, and they may provide the means for the design of novel gene targeted therapeutics (Hurley, 2002).

The strategy has been already used to target the *MDR1* gene obtaining inhibition of transcription as revealed by a meaningful reduction of mRNA amount (Scaggiante et al., 1994; Labroille et al., 1998; Morassutti et al., 1999). However, no detectable functional reversion of the drug was observed after TFO treatment. In the present study, we conceived, synthesized, and investigated for their biological activity new TFO conjugates of the anticancer drug DNM directed against *MDR1*. DNM belongs to the family of the anthracyclins, which are among the most commonly used and effective anticancer drugs; they are used in breast cancer, lymphomas, and mainly in acute leukemias (Hande, 2003). In the past, TFO conjugates of anthracycline derivatives have been synthesized to target an oligopyrimidine-oligopurine sequence in exon 2 of *MDR1* (Garbesi et al., 1997; Capobianco et al., 2001), and, recently, in the P2 promoter of *c-myc* (Carbone et al., 2004; Napoli et al., 2006). It is noteworthy that DNM is also the target of the P-gp pump, and, upon overexpression of *MDR1*, resistance to DNM is observed, which is very hampering for its use in chemotherapy. In a general effort to reverse multidrug resistance and to find more active and specific anticancer drugs, we show here for the first time that it is possible to combine (and take advantage of) three different properties of DNM conjugates: 1) DNM biological activity, 2) oligonucleotide chemical properties, and 3) ability of the TFO to specifically inhibit gene expression. These three properties allowed us to 1) inhibit the efflux of DNM conjugates from resistant cells (cells overexpressing the gene *MDR1*) and at the same time to 2) reduce the expression of both P-gp mRNA and protein levels in these cells. We exploited the oligopyrimidine-oligopurine tract in exon 3 of the *MDR1* gene described previously (Scaggiante et al., 1994; Labroille et al., 1998; Morassutti et al., 1999), and we conceived modified DNM oligonucleotides able to specifically target this sequence. The use of different types of oligonucleotides (parallel and antiparallel) containing different chemical modifications, such as thymidines substituted by 5-propynyluracils (P), cytosines substituted by 5-methylcytosines (M), and locked nucleic acids (LNAs), allowed us to choose the best chemistry to obtain a stable triplex. DNM was coupled to oligonucleotides, forming stable triple helices on the sequence target, and they efficiently inhibited P-gp expression. Furthermore, we studied the conditions allowing the accumulation of the conjugates in cell nuclei by imaging and microspectrofluorescence. Upon use of DNM-resistant cell lines, we show that the DNM/TFO conjugates are able to pass the cell membrane, remain in DNM-resistant cell lines, and inhibit the expression of *MDR1* gene.

Materials and Methods

Methods. For all oligonucleotide conjugates, mass determination was accomplished by electrospray ionization on a QSTAR pulsar I (Applied Biosystems, Courtaboeuf, France) and HPLC purifications were performed on an Agilent 1100 series system (Agilent Technologies, Massy, France) using a Xterra reversed-phase C18 column (4.6 × 50 mm; 2.5 μm). Absorbance spectrophotometry was performed on a Uvikon 860 (Kontron Instruments, Watford, Herts, UK).

Materials. All chemicals were purchased from Aldrich Chemical Co. (Milwaukee, WI). All solvents were of analytical grade.

Oligonucleotides. Oligonucleotides PM, PM-NH2, SC, and GT1–4 were purchased from Eurogentec (Seraing, Belgium). LNA1 to 3 were purchased from ProOligo (Hamburg, Germany). Concentrations were determined spectrophotometrically at 25°C using molar extinction coefficients at 260 nm calculated from a nearest-neighbor model (Cantor et al., 1970). PM-NH2 contains a $(CH_2)_6$-NH_2 linker at its 3′ end. SC of sequence 5′-MMPMMPPMMMMPMMM-3′ was coupled with the same procedure as PM to DNM at its 3′ end. si1 was an siRNA targeting the human *MDR1* mRNA at the level of region 88 to 108 relative to the start codon (antisense, 5′-UACACUGACAGUUGGUUUCdTdT-3′; sense, 5′-GAAACCAACUGUCAGUGUAdTdT-3′) (Stierlé et al., 2004, 2005). An all-phosphorothioate antisense (AS) oligonucleotide, 5′-d(CCATCCCGACCTCGCGCTCC-3′), was directed toward the region of the start codon (−16/+3) (Alahari et al., 1996; Brigui et al., 2003).

Synthesis. Daunomycin-conjugated oligonucleotides PM, SC, and LNA2, with a hexamethylene bridge connecting the 5′ end of the oligonucleotides to the *O*-4 position in the D ring of the anthraquinone, were synthesized accordingly to a procedure described previously (Capobianco et al., 2005). The iodoalkyl derivative of daunomycin was initially prepared with the amino group of daunomycin protected as trifluoroacetate. Synthesis of the daunomycin-conjugated oligonucleotides was then accomplished by reaction of the iodoalkyl derivative of daunomycin with phosphodiester oligonucleotides carrying a 3′- or 5′-thiophosphate group. After extraction of the excess of iodoalkyl derivative, the trifluoroacetyl protecting group was removed from the amino group of the daunomycin by mild basic hydrolysis. The daunomycin-conjugated oligonucleotides were then purified by reverse-phase HPLC. The structure of conjugates was confirmed by MS and UV-visible spectroscopy. A mean yield of 65% was obtained: PM-DNM MS (ES^-) m/z: 5452 $[M\text{-}H]^-$ (calculated: 5453); DNM-PM MS (ES^-) m/z: 5448 $[M\text{-}H]^-$ (calculated: 5453); and SC-DNM MS (ES^-) m/z: 5277 $[M\text{-}H]^-$ (calculated: 5278)

Gel Retardation Assay. The oligopyrimidine strand of the duplex was 5′ end-labeled with [α-^{32}P]ATP (GE Healthcare, Chalfont St. Giles, Buckinghamshire, UK) by T4 polynucleotide kinase (New England Biolabs, Ipswich, MA) according to the manufacturer's instructions. Increasing concentrations (10 nM–5 μM) of the triplex-forming oligonucleotides were added to 10 nM concentrations of the radiolabeled duplex in 10 mM $MgCl_2$, 50 mM NaCl, 50 mM HEPES, pH 7.2, 10% sucrose, and 0.5 mg/ml tRNA followed by sample incubation at 37°C for 2 to 48 h. Electrophoresis was performed on a nondenaturing 15% polyacrylamide gel containing 10 mM $MgCl_2$ and 50 mM HEPES, pH 7.2, at 37°C. To quantify the formation of the triplex, gels were scanned with a Typhoon 9410 (GE Healthcare). The concentration of conjugate or TFO necessary to obtain 50% of formed triplex (C_{50}) was calculated, and a mean value corresponding to three to five different experiments is reported.

UV Melting Experiments. A Uvikon 940 spectrophotometer (Kontron Instruments) with 1-cm optical pathlength quartz cuvettes was used to study thermal denaturation and renaturation of triplex formation. The cell holder was thermoregulated by an 80% water/20% ethylene glycol circulating liquid. Sample temperature was decreased from 60°C to 0°C, and then it was increased back to 60°C at 0.2°C/min, with absorption readings at 245, 260, 295, 520, and 620 nm taken every 1 to 1.2°C during three cycles. Samples were maintained at each extreme temperature for an additional 10 min. Experimental conditions were as described in the figure and table legends. All samples contained 10 mM sodium cacodylate at the indicated pH, 50 mM NaCl, and 10 mM $MgCl_2$. Oligonucleotides concentration was 1 μM R, 1.05 μM Y, and 1.2 μM TFO in the triplex experiments.

Cells and Transfection. MCF7-S (the parental human mammary adenocarcinoma cell line) and MCF7-R (the doxorubicin-resistant line) were a gift from M. F. Poupon (Institut Curie, Paris, France). NIH-3T3 cells were obtained from the American Type Culture Collection (Manassas, VA). NIH-MDR-G185 cells stably transfected with a plasmid containing the human *MDR1* gene (pSK1 MDR) were a gift from M. Gottesman (National Cancer Institute, Bethesda, MD). Cells were grown in RPMI 1640 medium supplemented with 10% decomplemented fetal bovine serum, 50 U/ml penicillin, 50 μg/ml streptomycin, and 2 mM glutamine in a 5% CO_2 atmosphere. Transfection with Oligofectamine (OFA) (Invitrogen, Paisley, UK) or SuperFect (QIAGEN, Hilden, Germany) was carried out as directed by the manufacturers. Cells (3×10^5/well) were plated in six-well plates. They were transfected at 30 to 40% confluence. The final concentrations in oligonucleotide were 500 nM for TFOs or AS and 10 nM for siRNA.

Fluorescence Imaging and Microspectrofluorometry. MCF7-R or NIH-3T3 cells were washed with ice-cold phosphate-buffered saline (PBS), and then they were observed by fluorescence microscopy on an Optiphot-2-epifluorescence microscope (Nikon, Tokyo, Japan) 24, 48, or 72 h after treatment with the DNM conjugates (alone or transfected with OFA). Nontransfected MCF7-S and MCF7-R were incubated with DNM (0.5 μM for 1 h), and then they were used as positive and negative controls of DNM incorporation. Images were detected with a cooled charge-coupled device camera (Micromax; Scientific Instruments, Monmouth Junction, NJ) with a 12-bit detector (RTEA-1317K; Eastman Kodak, Rochester, NY). A standard rhodamine filter set was used. Analysis was performed using IPLab software (Scanalytics, Fairfax, VA).

Forty-eight or 72 h after treatment, the location of DNM conjugates inside the cells was evaluated with a UV-visible microspectrofluorometer confocal prototype developed in our laboratory (Sureau et al., 1990). The excitation was the 488-nm wavelength of an argon laser (Spectra Physics, San Jose, CA). The beam power was reduced to 0.1 μW by the use of neutral density filters. The integration time of spectrum was 1 s. A water immersion 63× objective was used.

Western Blotting. Cells were lysed 72 h after transfection. Nontreated MCF7-R cells were used as reference of resistant cells. Cells were trypsinized, washed in PBS, counted, and resuspended in radioimmunoprecipitation assay lysis buffer (50 mM Tris-HCl, pH 7.5, 150 mM NaCl, 0.1% SDS, 1% Nonidet P-40, 0.5% deoxycholate) containing 5 mM EDTA and protease inhibitors (phenylmethylsulfonyl fluoride, leupeptin, and aprotinin) at the ratio of 100 μl of buffer for 3×10^6 cells. After 30 min on ice with some vortexing, the lysates were centrifuged at 13,000*g* for 20 min at 4°C. Protein concentration was determined with a protein assay kit (Sigma, Paris, France). Equal amounts of proteins (20 μg) were mixed with SDS reducing buffer. Protein samples were separated on 7.5% acrylamide SDS-polyacrylamide gel electrophoresis, and then they were transferred onto polyvinylidene difluoride membrane (Hybond-P; GE Healthcare). The membrane was blocked with 5% nonfat dry milk in 0.1% Tween/PBS, and then they were treated with 0.65 μg/ml C219 monoclonal anti-P-gp antibody (Dako Denmark A/S, Glostrup, Denmark) or 2 μg/ml AC-74 monoclonal anti β-actin antibody (Sigma). Detection by enzyme-linked chemiluminescence was performed according to the manufacturer's protocol (ECL Plus; GE Healthcare). P-gp expression was quantified by NIH Image software (http://rsb.info.nih.gov/ij/).

Reverse Transcription-Polymerase Chain Reaction. Total RNA was extracted (RNeasy kit; QIAGEN) 48 and 72 h after transfection of MCF7-R cells, and cDNA was synthesized using Omniscript reverse transcription kit (QIAGEN) and 0.5 μM gene-specific reverse primer of *MDR1* or β-actin, which was chosen as an internal control. PCR Master Mix (MBI Fermentas, Hanover, MD) was used for DNA amplification, which was kept in its exponential phase (23 cycles). Primers used for *MDR1* amplification (0.5 μM) were as follows: sense, 5′-d(TCTTGAAGGGCCTGAACCTG-3′) and reverse, 5′-d(AGTCATAGGCATTGGCTTCC-3′). The 300-nucleotide amplified region was located on exons 12 and 13. Primers for β-actin amplification (0.3 μM) were as follows: sense, 5′-d(ACCAACTGGGACGACATGGA-3′) and reverse, 5′-d(CTCCTTAATGTCACGCACGA-3′). Amplicon length is 237 nucleotides. Amplification products were separated on a 1.8% agarose gel stained with 6 μg/ml ethidium bromide. Gene expression level was quantified by NIH Image software.

Results

Choice of the Target Site and TFOs. To choose a site to form a triple helix, the *MDR1* gene was screened with BLAST (http://www.ncbi.nlm.nih.gov/BLAST/) for oligopurine-oligopyrimidine sequences. In the whole gene, three regions are susceptible to form a stable triple helix: 1) a 12-bp region in exon 2, 2) a 21-bp region in exon 3, and 3) a long sequence of 410 bp in intron 14 (Fig. 1A) (Chen et al., 1990; Pauly et al., 1995). The sequence of exon 2 containing only 12 bp was judged too short in view of the specificity of action of the TFOs. Therefore, the oligopurine-oligopyrimidine sequence located in exon 3 and illustrated in Fig. 1B was chosen as the target for TFOs and DNM conjugates. This sequence contains an inverted site that has to be taken into account during the conception of new and efficient TFOs.

TFOs form Hoogsteen or reverse Hoogsteen hydrogen bonds with the purine-rich strand of the duplex DNA (Buchini and Leumann, 2003). Purine-rich (GA) and mixed purine/pyrimidine (GT) TFOs bind preferentially antiparallel to the purine-rich strand, whereas pyrimidine-rich (TC) TFOs bind parallel. In both parallel and antiparallel triplex motif, the TFO is located in the major groove of the double helix. GA and GT TFOs form stable triplexes at physiological pH, whereas the ability of TC TFOs to form stable triplexes at neutral pH is very limited, because of the required protonation of the cytosines to form the C·G*C^+ triplets. However, it is possible to introduce chemical modifications in the structure of the oligonucleotide that improve the stability of the formed triplex and allow triplex formation at neutral pH (Buchini and Leumann, 2003).

The TFOs chosen to target the selected sequence in exon 3 are reported in Fig. 1C. Several oligonucleotides, with or without chemical modifications, have been conceived. Four TFOs with (GT) motif were chosen in the aim to avoid pH dependence. The oligonucleotide indicated as GT1 corresponds to the oligonucleotide used in a previous study, and it contains a single base interruption in the purine strand (indicated in bold in the duplex sequence) (Scaggiante et al., 1994). Oligonucleotides GT2 and GT3 encompass together GT1, and they are in the parallel orientation. GT2 covers the region with the single base interruption in the purine strand. GT4 has been chosen to form an antiparallel triplex. Furthermore, (TC) oligonucleotides (directed against box a, Fig. 1) were used, and two types of modifications were introduced to increase triplex stability. In PM, thymidines are substituted by 5-propynyl-deoxyuridine (P) and cytosines by 5-methyl-deoxycytidine (M). These two modifications are already known to stabilize the triplex (Duca et al., 2005). Finally, LNA have been studied (Fig. 1D). Oligonucleotides LNA1, LNA2, and LNA3 alternate T, M, LNA-modified thymidines (T in Fig. 1), or cytidines (C in Fig. 1) that have been shown to improve triplex formation at physiological pH (Sun et al., 2004).

Triplex Formation. At first, we studied the ability of the described oligonucleotides to form a triple helix by using both

gel retardation assays and UV-visible absorbance melting experiments. In our experimental conditions, the (GT) oligonucleotides (GT1–4) are unable to form a triple helix even at high concentrations (10 μM) and long incubation times (up to 48 h). All other chosen oligonucleotides (PM and LNA1–3) are able to form a triple helix, with different efficacies. As shown in Fig. 2, A and B (top), after 2-h incubation at 37°C, oligonucleotide PM was the most efficient in forming the triplex. LNA1 and LNA2 are slightly less efficient, whereas LNA3 has the lowest ability to form the triplex. Figure 2, A and B (bottom), shows the gel retardation assay after 24 h of incubation at 37°C, and we can observe that the efficacy of all oligonucleotides is comparable. These results are summarized in Table 1, where both C_{50} values and melting temperature (T_m) values are reported. Melting temperatures values for all these oligonucleotides do not present relevant differences, but the small variations correspond well to the differences recorded by gel shift assays. Observed values of K_d and T_m are in good agreement with what reported for the same type of modified triplex-forming oligonucleotides in similar experimental conditions (Sun et al., 2004). To further compare these four oligonucleotides, we studied the kinetic of formation of the triple helix over 48 h. As reported in Fig. 3, PM and LNA1 to 3 formed triplexes of comparable stability after 48 h, but the rate of formation is different. Triplex formation is faster for the PM oligonucleotide. Based on these observations, the study was pursued coupling PM and LNA2 oligonucleotides to DNM to perform cellular experiments.

Synthesis of the Daunomycin-Conjugated TFOs. PM and LNA2 have been coupled to DNM in 3′ position, leading to conjugates PM-DNM and LNA2-DNM (Fig. 4). The presence of DNM at the 3′ end of the oligonucleotides protects them against exonuclease degradation in cells. Furthermore, it is well established that for pyrimidine triplexes the conjugation in 5′ of DNA intercalators, such as acridine (Sun et al., 1989; Birg et al., 1990) or more recently DNM (Garbesi et al., 1997; Carbone et al., 2004; Napoli et al., 2006), stabilizes triplex formation. For this reason, PM has been coupled to DNM also in 5′ position, resulting in DNM-PM. In the latter case, the oligonucleotide was protected in 3′ position toward exonuclease degradation by introduction of an amino group [$(CH_2)_6$-NH_2] instead of the terminal phosphate group. As negative control, daunomycin was coupled to the 3′ end of another oligonucleotide (SC) (the sequence is reported under *Materials and Methods*) that is unable to form a triple helix on the desired *MDR1* sequence (conjugate SC-DNM).

For the synthesis of the conjugates, as shown in Fig. 4, TFOs were coupled to an ω-iodoalkyl derivative of daunomycin, whose synthesis was described previously (Capobianco et al., 2005). In the first step, the thiophosphate group of the oligonucleotide is activated by a 0.5 M solution of dithiothreitol and crown ether 18-crown-6 in *N*,*N*-dimethylformamide. The coupling is fol-

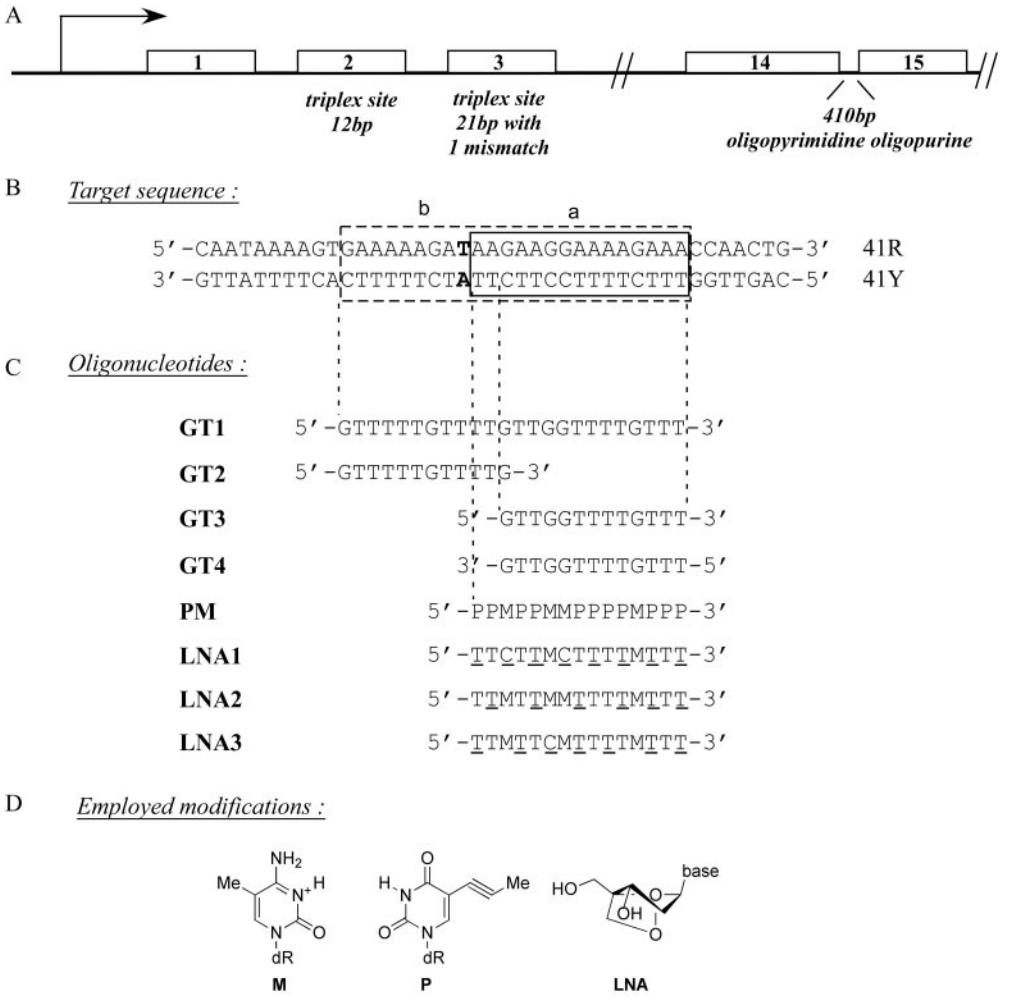

Fig. 1. A, potential triplex sites in the *MDR1* gene. B, oligopurine-oligopyrimidine sequence within exon 3 of *MDR1* gene. The 15-bp target sequence (a) is encircled by a continuous line. A longer 24-bp region containing an inverted site (bold bases) is indicated by a dotted line (b). C, oligonucleotides used to study triplex formation against region a. D, base and sugar modifications used in this study.

lowed by the deprotection of the DNM moiety using a 0.2 M solution of NaOH. After HPLC purification, the product has been obtained in 65% yield over two steps.

Once synthesized, the stability of the formed triplex was evaluated by gel shift assay (Table 2; Supplemental Fig. 1). As expected, the coupling of DNM to the 5′ end of the TFO (DNM-PM) induced a stabilization of the triplex compared with PM alone. This is probably due to the intercalation of the DNM moiety at the 5′ end of the triplex, as observed in previous work with various acridine-conjugated oligonucleotides analogs (Arimondo et al., 2000) and other GT and TC triplex-forming oligonucleotides (Capobianco et al., 2001; Carbone et al., 2004; Napoli et al., 2006). Noteworthy, the presence of the intercalating agent at the 5′ end of the TFO speeds up triplex formation (Fig. 5). The attachment of the DNM moiety to the 3′ end of the TFO (PM-DNM), both in the case of the PM and LNA2 oligonucleotide, induces a destabilization of the triple-helical structure, which is in agreement with previous findings with acridine-TFO conjugates, suggesting marked differences between the 5′ and 3′ triplex/duplex junction (Sun et al., 1989; Arimondo et al., 2000). This destabilization effect is more pronounced for LNA2-DNM (Table 2).

Cellular Uptake of PM-DNM. After the synthesis of TFO-DNM conjugates, we turned our attention to their application in the cellular context. The first question we wanted to address was the cellular uptake in *MDR1*-resistant cells of conjugated DNM compared with free unconjugated DNM. We chose for these experiments to use PM-DNM, which is protected from exonuclease degradation in 3′ by the DNM moiety. To our knowledge, 3′ DNM conjugates have not been studied previously.

MCF7-S cells (the parental cell), MCF7-R cells (the doxorubicin-resistant line), parental NIH-3T3, and resistant NIH-MDR-G185 overexpressing the human *MDR1* gene were treated for 1 h with 0.5 μM DNM, and then they were examined under a fluorescence microscope. MCF7-S cells were highly fluorescent, with a predominant accumulation of DNM in the nucleus (Fig. 6A), whereas no fluorescence was observed in MCF7-R cells. As expected, high cell surface expression of P-gp in resistant MCF7-R cells leads to DNM efflux. Similar results were obtained with NIH-3T3 and NIH-MDR-G185 cells (data not shown).

After this control experiment, the cellular uptake of 0.5 μM PM-DNM or LNA2-DNM in MCF7-S cells, MCF7-R cells, NIH-3T3, and NIH-MDR-G185 cells was followed by fluorescence imaging at 24, 48, and 72 h. Figure 6B shows the results obtained after treatment of MCF7-R cells with PM-DNM conjugate alone (first column), with PM-DNM conjugate and OFA (a cationic lipid formulation) as transfectant agent (second column), and with PM-DNM conjugate and SuperFect (a cationic dendrimer) as transfectant agent (third

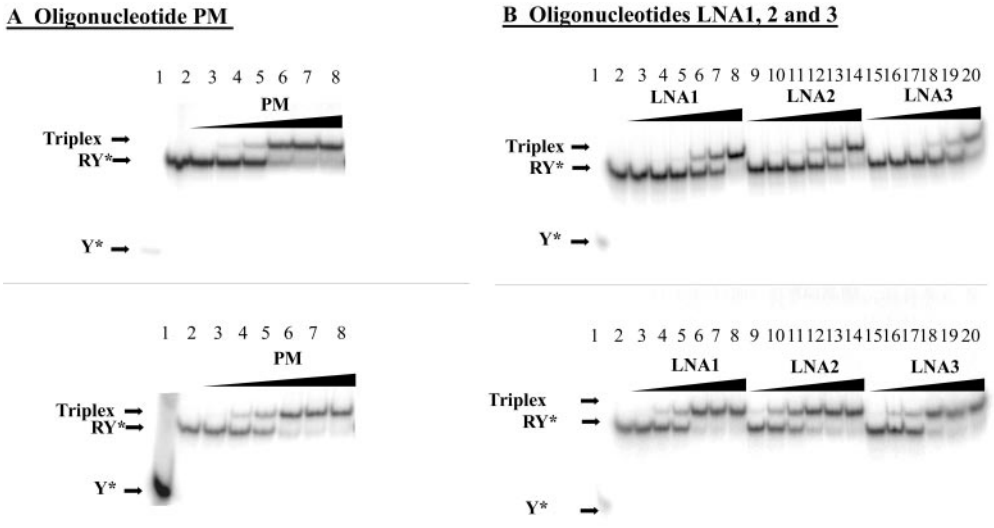

Fig. 2. Gel retardation assays obtained after 2 h (top) and 24 h (bottom) of incubation at 37°C in 50 mM HEPES, pH 7.2, 50 mM NaCl, and 10 mM $MgCl_2$. A, lane 1, radiolabeled Y strand; lane 2, radiolabeled duplex RY; and lanes 3 to 8 duplex RY incubated with TFO PM at 0.01, 0.05, 0.1, 0.5, 1, and 5 μM, respectively. B, lane 1, radiolabeled Y strand; lane 2, radiolabeled duplex RY; lanes 3 to 8, duplex RY incubated with TFO LNA1 at 0.01, 0.05, 0.1, 0.5, 1, and 5 μM, respectively; lanes 9 to 14, duplex RY incubated with TFO LNA2 at 0.01, 0.05, 0.1, 0.5, 1, and 5 μM, respectively; and lanes 15 to 20, duplex RY incubated with TFO LNA3 at 0.01, 0.05, 0.1, 0.5, 1, and 5 μM, respectively.

TABLE 1

C_{50} and T_m values for triple helix formation of the studied oligonucleotides

C_{50} values were calculated by gel shift assay after 2- and 24-h incubation at 37°C in 50 mM HEPES, pH 7.2, 50 mM NaCl, and 10 mM $MgCl_2$. T_m values were obtained by absorbance measurements (220–450 nm) in function of temperature (from 0°C to 80°C at 0.2°C/min) in 10 mM sodium cacodylate, pH 7.2, 10 mM $MgCl_2$, and 50 mM NaCl. Underlined bases are LNA bases.

	Oligonucleotide (5′–3′)	C_{50}		T_m
		2 h	24 h	
		μM		°C
GT1	5′-GTTTTTGTTTTGTTGGTTTTGTTT-3′	None	None	No
GT2	5′-GTTTTTGTTTTG-3′	None	None	No
GT3	5′-GTTGGTTTTGTTT-3′	None	None	No
GT4	5′-TTTGTTTTGGTTG-3′	None	None	No
PM	5′-PPMPPMMPPPPMPPP-3′	0.46 ± 0.07	0.05 ± 0.01	49 ± 0.5
LNA1	5′-TTCTTMCTTTTMTTT-3′	0.87 ± 0.10	0.12 ± 0.05	47 ± 0.5
LNA2	5′-TTMTTMMTTTTMTTT-3′	0.67 ± 0.11	0.06 ± 0.02	47 ± 0.5
LNA3	5′-TTMTTCMTTTTMTTT-3′	1.4 ± 0.2	0.08 ± 0.01	46 ± 0.5

column). Because of the important cell mortality observed as soon as 24 h after treatment with LNA2-DNM, we chose PM-DNM to pursue the cellular study. The first remarkable observation derived from the comparison of Fig. 6, A and B, is that PM-DNM conjugate is able to entry in resistant cells, with or without transfectant agent. This shows that, in contrast to DNM alone, the oligonucleotide confers to DNM the ability to overcome cellular resistance (i.e., the efflux activity of the Pg-P pump). Similar results were obtained for NIH-MDR-G185 cells (Supplemental Fig. 2). No significant differences in intensity or intracellular distribution of the DNM-conjugated oligonucleotides were observed between parental and resistant cells. The second noteworthy observation is that the hydrophobicity of the anthraquinone moiety of DNM increases the affinity of the conjugate for the cell membrane and helps the uptake of the conjugates by endocytosis. In fact, even in the absence of a transfectant agent the conjugate is able to enter the cell membrane, a result very difficult to obtain for an oligonucleotide alone. The two moieties that constitute the conjugate, the anthracycline and the TFO, thus act synergistically and favor cell penetration. It is then conceivable that, when coupled to an oligonucleotide, DNM can bypass cell resistance and still exert some form of anticancer effect.

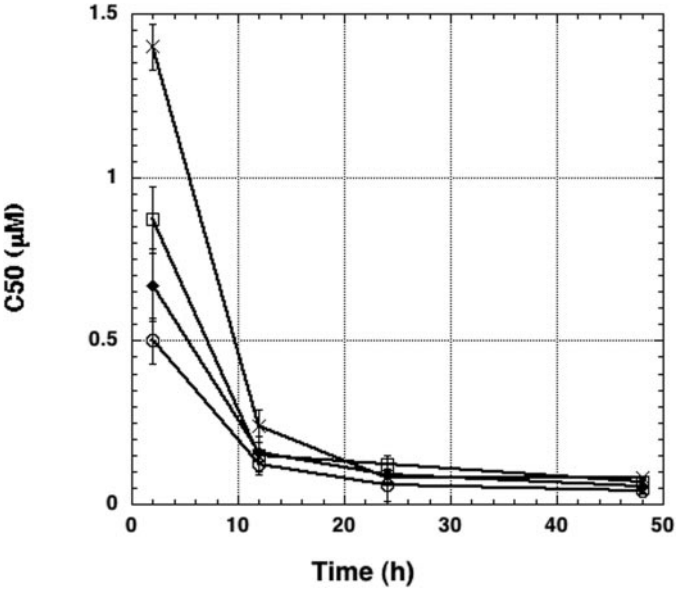

Fig. 3. Graph reporting the kinetic of the formation of triple helix with the selected DNA sequence by oligonucleotides PM (circles), LNA1 (diamonds), LNA2 (crosses), and LNA3 (squares) over 72 h of incubation at 37°C in 50 mM HEPES 50, pH 7.2, 50 mM NaCl, and 10 mM $MgCl_2$. The error bars indicate the standard deviation.

Regarding the cellular distribution of PM-DNM in cells, this is very different from the distribution of DNM. Whereas DNM has been shown to accumulate in nuclei (Fig. 6A), PM-DNM is largely localized in cytoplasm with perinuclear accumulation (Fig. 6B). Furthermore, the presence of fluorescent vesicles can be observed, suggesting the involvement of an endocytic pathway in the internalization of the conjugates (Tonkinson and Stein, 1994; Hu et al., 2002). Whereas anthracyclines quickly accumulate in cell nuclei, and in a smaller proportion in organelles (Rutherford and Willingham, 1993), oligonucleotides initially incorporate into endosomes, and they are localized in the nucleus much later after their release into the cytoplasm. In agreement with our results, 5′ DNM conjugates of an 11-mer (GT) TFO have been shown to accumulate primarily in the cytoplasm of MCF7-S cells in the absence of transfectant (Carbone et al., 2004). We suggest that, in the PM-DNM, the DNM moiety allows cell internalization of the conjugates into parental as well as resistant cells, whereas the oligonucleotide moiety is responsible of the cytoplasmic localization of PM-DNM.

As shown in Fig. 6B, the cell fluorescence intensity 24 h after transfection of PM-DNM into MCF7-R cells in the presence of OFA or SuperFect is comparable with the intensity without transfectant. However, fluorescent speckles are now observable (indicated by an arrow). In the presence of transfectant, some conjugates are trapped in vesicles as reservoirs of PM-DNM, which are released over time. After 48 h, there is an enhancement in the fluorescence intensity of cells that have been transfected in the presence of the transfectant agent. Their speckled pattern is also increased. A cationic lipid-mediated uptake has already been shown in nonresistant cells to increase the intracellular pool of 5′ DNM conjugates (Carbone et al., 2004), with a corresponding increase in nuclear accumulation. Here, we also used a cation dendrimer agent and observed the same effect. Finally, 72 h after transfection, cells are observed at 63× magnification, and nuclear fluorescence is observed when PM-DNM is transfected in the presence of OFA. Nevertheless, the nuclear fluorescence quenching of DNM (DNM fluorescence decreases 20 time after its intercalation in DNA) (Laigle et al., 1996) is a limitation for fluorescence imaging. Microspectrofluorimetry allowed the nuclear localization of PM-DNM as soon as 48 h after transfection with OFA, as confirmed in Fig. 7A. A large

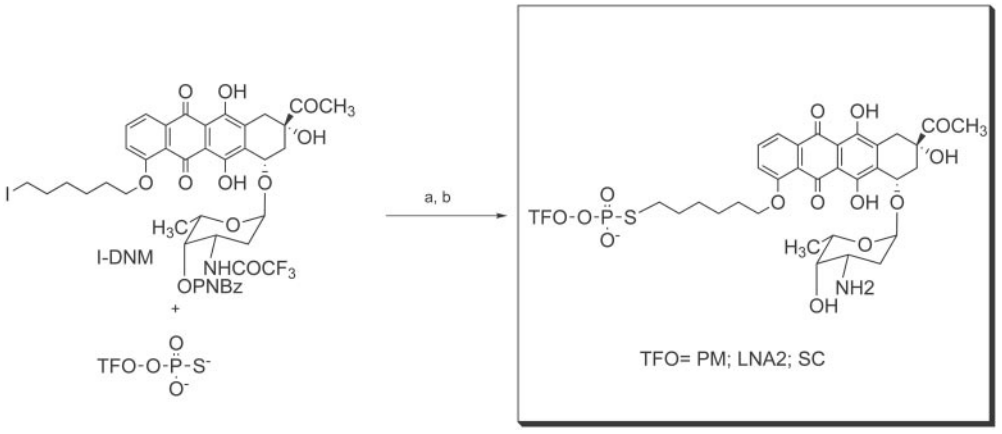

Fig. 4. Synthesis of daunomycin conjugates. Reagents were dithiothreitol, 18-crown-6, and *N*,*N*-dimethylfomamide (a) and 0.2 M NaOH (b). Chemical structure of the conjugates are shown.

band centered around 596 nm is observable. Very little nuclear accumulation was measured in the absence of OFA. In that case, similar spectra were observed in the cytoplasm and in the nucleus (Fig. 7C, two bands around 560 and 590 nm), which resemble the spectrum recorded in the cytoplasm when the transfecting agent OFA is used (Fig. 7B). DNM presents two major emission maxima at ~560 and ~592 nm ($I_{560\ nm}/I_{592\ nm}$ = 0.8) (Karukstis et al., 1998). The peak at ~592 nm dramatically increased in the DNM conjugates (the spectrum of PM-DNM in PBS is reported in Fig. 7D for comparison). In contrast, inversion of the 560-nm/592-nm intensity ratio has been observed in relation to doxorubicin degradation (Fiallo et al., 1993). Therefore, the enhancement of the peak at ~560 nm in the cytoplasm when using OFA (Fig. 7B) or in both nucleus and cytoplasm in its absence (Fig. 7C) might indicate a degradation of the conjugate with liberation of free DNM. However we did not succeed to reproduce this potential degradation of the conjugates in vitro in cell lysates or in various cell media in the absence or presence of salmon sperm DNA. It is noteworthy that no free DNM was detected in the nucleus when OFA was used as transfectant (Fig. 7A). In that case, the enlargement of the fluorescence peak observed in the nucleus (Fig. 7A) in comparison with the peak of the conjugate in PBS (Fig. 7D) can result from a 10-nm blue shift that we observe when PM-DNM is incubated in the test tube with cell lysates (data not shown). Similar results were obtained with NIH-MDR-G185 cells and with the nonspecific 3′ DNM conjugate SC-DNM (data not shown).

Down-Regulation of MDR1 Gene Expression with the Triplex-Forming PM-DNM. With the experiments described above, we have established that the PM-DNM and DNM-PM conjugates form a stable triplexes on the DNA target (Table 2) and that they are less cytotoxic than LNA2-DNM. Furthermore, when transfected in the presence of OFA, they accumulate in the nucleus of resistant cells, and they are not ejected by the P-gp pump (Figs. 6 and 7). Thus, we wanted to investigate whether the conjugates are able to reach their target (the *MDR1* gene) and modulate its expression.

The ability of PM-DNM and DNM-PM to down-regulate the *MDR1* expression in MCF7-R cells was studied at the level of the protein and the mRNA by Western blot and RT-PCR, respectively (Fig. 8). An efficient siRNA (si1) (Stierlé et al., 2004, 2005) and an AS (Brigui et al., 2003) directed against *MDR1* were chosen as positive controls. SC-DNM (a scrambled control of PM-DNM) and PM-NH2 [PM containing the linker arm $(CH_2)_6$-NH_2 in 3′ and no DNM] were used as negative controls. We have previously shown that with si1 the decrease in P-gp levels in MCF7-R cells is best followed after 72 h of treatment, whereas the highest reduction in *MDR1* mRNA was obtained after 48 h (Stierlé et al., 2004).

TABLE 2

C_{50} values for triple helix formation of the DNM conjugates

C_{50} values were calculated by gel shift assay after 2- and 24-h incubation at 37°C in 50 mM HEPES, pH 7.2, 50 nM NaCl, and 10 mM $MgCl_2$.

Oligonucleotide	C_{50}	
	2 h	24 h
	μM	
PM-DNM	0.83 ± 0.07	0.19 ± 0.10
LNA2-DNM	1.0 ± 0.3	0.39 ± 0.09
DNM-PM	0.38 ± 0.07	0.04 ± 0.01

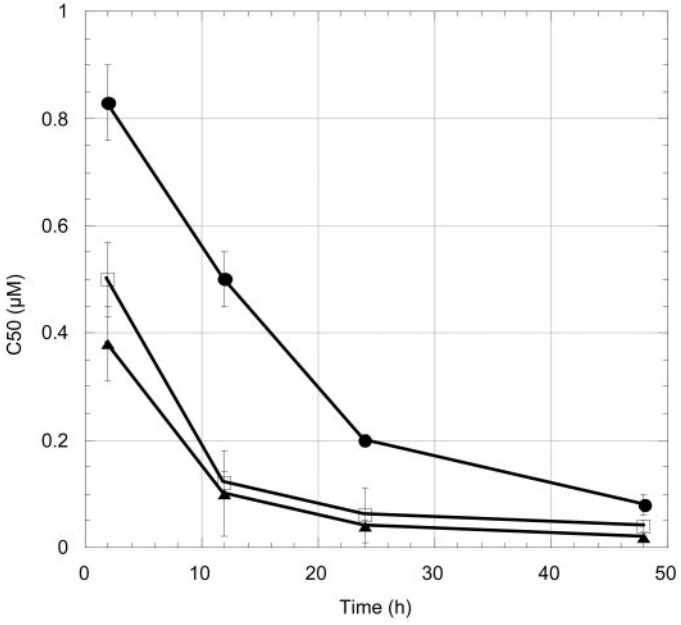

Fig. 5. Graph reporting the kinetics of the formation of triple helix with the conjugates oligonucleotides over 72 h of incubation at 37°C in 50 mM HEPES, pH 7.2, 50 mM NaCl, and 10 mM $MgCl_2$. PM-DNM (●), DNM-PM (▲), and PM as control (□). The error bars indicate the S.D.

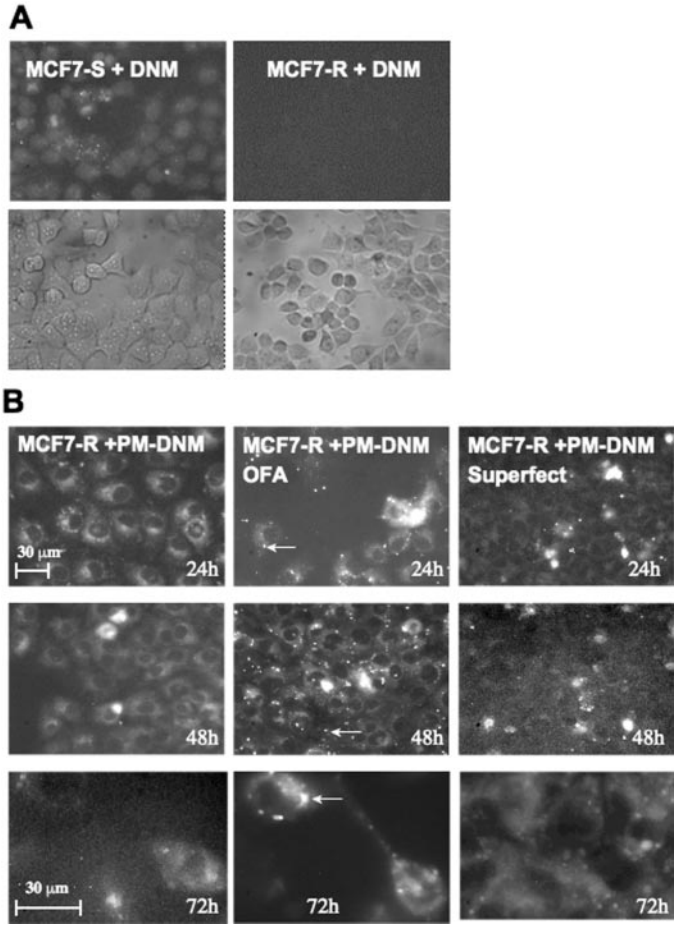

Fig. 6. Fluorescence imaging. A, 0.5 μM DNM in MCF7-S and MCF7-R cells after 1-h incubation (top, fluorescence; bottom, bright field). B, 0.5 μM PM-DNM in MCF7-R cells after 24-, 48-, or 72-h treatment without transfectant or transfected with OFA or with SuperFect.

This 24-h gap results from P-gp long half-life (Nieth et al., 2003; Stierlé et al., 2004). Therefore, we studied the effect of the conjugates on mRNA expression after 48 h of treatment and on P-gp levels after 72 h.

All oligonucleotides were used at a concentration of 500 nM, with the exception of si1 that was used at a concentration of 10 nM. Figure 8, A and B, shows the results obtained for P-gp and mRNA expression, respectively. Compared with the reference SC-DNM (unable to form triplex on *MDR1* gene), PM-NH_2 caused a slight decrease in P-gp (85% remaining signal), and it had no effect on mRNA (96% remaining signal) expression. Concerning the positive controls, si1 gave, as expected, a very efficient decrease of P-gp levels, with only 30% of signal observed, and mRNA expression (40% remaining). Again, treatment with the positive antisense control AS led to 68% P-gp expression remaining and 36% mRNA expression remaining. Regarding the conjugates, a significant decrease in P-gp expression (46% remaining) and mRNA (64% remaining) was obtained with PM-DNM, whereas DNM-PM gave only 75 and 88%, respectively. The conjugate containing the DNM residue in 3′ position is thus clearly more active in inhibiting *MDR1* gene expression than the residue in the 5′ position.

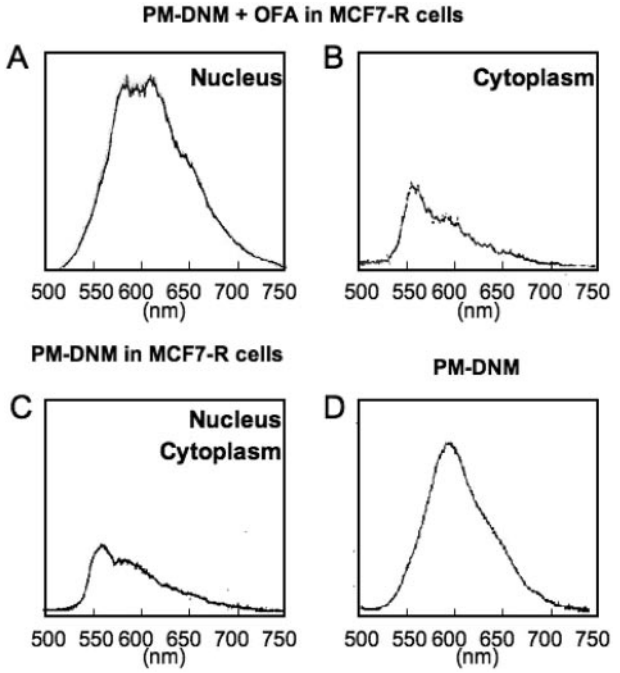

Fig. 7. Microspectrofluorometry ($\lambda_{excitation}$ = 488 nm) of 0.5 μM PM-DNM in MCF7-R cells after 48-h treatment. Top, with OFA. Fluorescence spectra recorded in the nucleus (A) and in the cytoplasm (B). Bottom, without OFA. Similar spectra were recorded in the nucleus or the cytoplasm (C). D, for comparison, 0.5 μM PM-DNM in PBS.

Discussion

Anthracyclines, and in particular DNM, are used for the treatment of a wide range of malignancies, but the emergence of multidrug resistance, as well as myelosuppression and cardiotoxicity, limits their effectiveness in the clinic. In this study, we demonstrate that it is possible to specifically target DNM to specific sites on the DNA, by using conjugates of oligonucleotides able to form a triple helix on the DNA and the DNM moiety. Moreover, the conjugation of DNM to the oligonucleotides was shown to improve their cellular uptake, and the DNM conjugates were able to deliver the drug on the *MDR1* gene even in DNM-resistant cells. In the literature, DNM has been coupled to several triplex-forming oligonucleotides and in particular to the 5′ end of an 11-mer (GT) TFO, which revealed to be highly specific for its target sequence, leading to reduction of transcription of c-myc in vitro and in cancers cells (Carbone et al., 2004; Napoli et al., 2006). Such 5′ conjugates showed a higher degree of affinity than native oligonucleotides for the oligopyrimidine-oligopurine duplex target, and the presence of the amino sugar of DNM increased such stability (Garbesi et al., 1997). In fact, in the DNM-TFO conjugates, the anthraquinone moiety intercalates in duplex DNA. Once intercalated in DNA, ring D of the anthraquinone protrudes into the major groove of DNA, whereas ring A reaches out into the minor groove. The amino sugar, which is linked to ring A, is therefore located in the minor groove and stabilizes the complex (Frederick et al., 1990).

In this study, we investigated three types of TFOs: 1) (GT)-containing oligonucleotides, 2) PM oligonucleotides (where thymidines have been substituted by P and cytosines

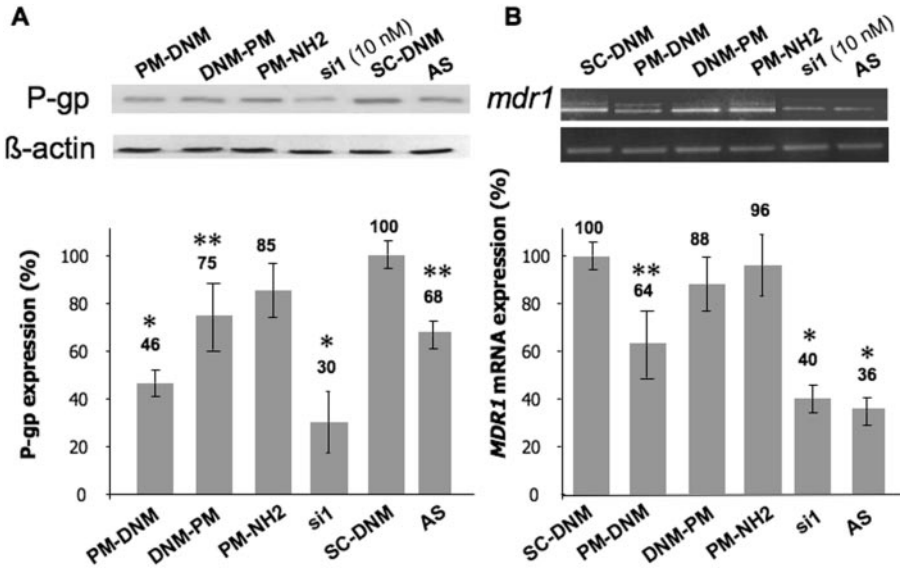

Fig. 8. *MDR1* expression after treatment with SC-DNM, PM-DNM, DNM-PM, PM-NH2, si1, and AS of MCF7-R cells transfected in the presence of OFA. [Oligonucleotides] = 500 nM, except [si1] = 10 nM. β-Actin was used as an internal control. A, Western blotting analysis at 72 h. Average of the remaining P-gp expression, including S.D. *, $p < 0.01$ compared with SC-DNM; **, $p < 0.05$. All experiments were performed at least in duplicate, and three Western blots were performed for each cell lysis preparation. B, RT-PCR analysis at 48 h. Average of the remaining P-gp expression, including standard deviation. *, $p < 0.01$ compared with SC-DNM; **, $p < 0.05$. Three transfection experiments have been performed, and PCR was in duplicate for each of them.

by M), and 3) LNA-containing oligonucleotides (Fig. 1). We were surprised to find that the (GT) TFOs did not form a triplex helix in our experimental conditions (pH 7.2; 37°C; 100 mM NaCl and 10 mM $MgCl_2$). The previously studied GT1 was, in fact, shown to form a stable triplex only in the presence of cationic spermidine and at 20°C (Scaggiante et al., 1994), conditions that favor triplex formation. In contrast, the pyrimidine chemically modified TFOs (PM and LNA) formed observable triplexes. The kinetics is different for the LNA-modified TFOs and the PM TFO, the latter being faster and more stable (2-fold; Fig. 3; Table 1). Among the LNA TFOs, the most efficient contains 5-methylcytosines instead of cytosines and alternated LNA thymines, starting with a non-LNA base in 5′. This is in agreement with previous observations indicating that the most stable LNA forming triplexes contain alternate LNA thymidines (every two to three bases) and 5-methylcytosines (Sun et al., 2004). Thus, among the eight oligonucleotides studied for their ability to form a triple helix, we found four of them (PM and LNA1–3) suitable to be used in an antigene approach. We finally chose PM and LNA2 for the conjugation to DNM because they were able to attain 100% of triplex formed rapidly (Figs. 2 and 3). Upon conjugation to DNM at the 3′ end, triplex stability decreased and also the kinetics of formation (Table 2). Coupling to the 5′ end stabilized triplex formation and increased the kinetics, confirming previous reports (Garbesi et al., 1997; Capobianco et al., 2001, 2005). However, the stabilization observed in our study is lower than observed previously. Noteworthy, the experiments are not comparable because, in the literature, in the absence of DNM the TFOs hardly formed a triplex in near physiological conditions, whereas, in our case, the TFO used already forms a very stable triplex on the target site. Thus, we cannot conclude whether there is a lower stabilization effect by DNM than expected and whether the lack of a CpG sequence at the intercalation site, preferred by DNM (Quigley et al., 1980; Capobianco et al., 2001), or structural variations of the triplex induced by the chemical modifications on the TFOs play any role. Concerning the difference in 3′ versus 5′ conjugation, our findings are in agreement with previous reports for acridine and (T,C) TFO conjugates (Sun et al., 1989, 1991). In brief, it has been observed that intercalating agents stabilize triplex formation when attached to the 5′ of pyrimidine TFOs and thus when positioned at the 5′ duplex/triplex junction. Because of the lack of a systematic study on antiparallel triplexes, it is not possible to compare our conjugates to the 5′ DNM-(GT) TFOs (3′ triplex/duplex junction) that were used for cellular studies (Carbone et al., 2004; Napoli et al., 2006).

On the cellular aspect, we observed, interestingly, that the PM-DNM conjugates are able to penetrate in the cells and to remain up to 72 h, in breast cancer-resistant MCF7-R cells and in the mouse fibroblasts NIH-MDR-G185 overexpressing *MDR1*, cells known to induce DNM efflux by the P-gp pump. It is noteworthy that the amount of fluorescence observed is 2 times higher than that of DNM alone. Therefore, the conjugates are able to enter resistant cells as a result of both the DNM moiety that increases the lipophilicity of TFO and the oligonucleotide moiety that is not recognized by the P-gp pump. The use of transfectant agents increases the penetration efficacy (2.3-fold), and it favors nuclear localization that increases up to 72 h, as described previously for the DNM-(GT) TFO in prostate cancer cells DU145 and PC3 (Carbone et al., 2004). Even if the use of transfectant was necessary to enhance TFO nuclear accumulation of the conjugates and therefore antigene effect, the fact that these conjugates overcome MDR resistance and are able to enter cells without transfecting agents and to remain up to 72 h makes them interesting tools to deliver DNM in drug-resistant cells, upon use eventually of a cleavable linker between the two entities. By microspectrofluorometry, we monitored the fluorescence spectra in the nucleus and in the cytoplasm of cells. Even if there might be a partial degradation of the conjugate with release of free DNM (as suggested by an enhancement of the shoulder at ~560 nm; Fig. 7), especially in the absence of the transfecting agent, we observe a clear peak at ~590 nm due to the intact conjugate, particularly in the nucleus (Fig. 7A). This intact conjugate is responsible for modulation of the expression of the target *MDR1* as observed by RT-PCR and Western blot (Fig. 8).

Noteworthy, in vitro studies showed that conjugation of DNM at the 5′ end of PM (DNM-PM) led to stabilization of the triplex and conjugation at its 3′ end (PM-DNM) to destabilization. In contrast, Western blot and RT PCR analysis revealed that, at the cellular level, PM-DNM is the most efficient: only 46% of *MDR1* expression was observed, compared with 75% with DNM-PM and 85% with PM-NH2. This is a clear indication that there is not always a correlation between triplex stability in vitro and the biological effect. The results here obtained seem to suggest that the DNM moiety of the conjugates plays an important and active role in the biological effect, regardless of its capacity of stabilizing the triple helix. The molecular mechanism of action in vivo of DNM is not completely elucidated, although it is known that its intercalation in the DNA double helix plays an essential role in the cytotoxic action. After intercalation, three mechanisms are conceivable: 1) topoisomerase II poisoning, by stabilizing the cleavage complex formed by the enzyme and DNA as amsacrine or epipodophyllotoxins (Baldwin and Osheroff, 2005); 2) DNA alkylation (Swift et al., 2006); and 3) generation of hydroxyl radicals responsible for double-stranded breaks of DNA. Furthermore, other possible mechanisms of action have been proposed recently (Gewirtz, 1999). We tested whether the mechanism of action of the conjugate could be due to sequence-specific topoisomerase II DNA cleavage (Supplemental Fig. 3). No sequence-specific DNA cleavage could be observed due to the action of the conjugates, even if it is clearly seen that the DNM is well positioned at the triplex end (a longer footprint is observed). We also controlled whether the difference could be due to an antisense effect of the TFO that can bind to the purine-rich RNA. We observed, in fact, that the TFOs bind to the RNA purine strand of the target sequence, especially LNA2 (C_{50} = 0.03 μM ± 0.01; Supplemental Fig. 4). This is not surprising because the LNA chemistry was developed to increase the stability of the antisense oligonucleotides. Finally, DNM-PM also forms a more stable duplex on the RNA purine strand of the target sequence (C_{50} = 0.04 ± 0.02, 0.06 ± 0.02, and 0.07 ± 0.01 μM for DNM-PM, PM, and PM-DNM, respectively), and this antisense effect cannot account for the inhibition of *MDR1* that is observed in cells. We also excluded the degradation of DNM-PM conjugate, which is protected in the 3′ by the presence of a $(CH_2)_6$-NH_2 linker arm; in cells, both conjugates are stable up to 72 h (data not shown). Together, these results indicate, for the first time, an active role of DNM in the biological effect of the conjugates, which it is not related to a pure binding effect, regardless of the mechanism of action

(e.g., DNA damage, topoisomerase poisoning, or impaired DNA repair). The difference 5′ versus 3′ can be explained in part by the different way of intercalation of the DNM at the two junctions, and thus a different orientation/availability of the drug for its action, with the 5′ junction being presumably more prone to intercalation. The neighboring sequences may also influence the activity of DNM (ATA/TAT in 5′ versus ACC/TGG in 3′); it has been shown, for example, that DNM lesions are induced principally 5′ of GpC (Swift et al., 2006).

In conclusion, we found that upon conjugation between the anticancer drug DNM and *MDR1*-directed TFOs it is possible to 1) bypass multidrug resistance, rendering DNM conjugates immune to P-gp action (oligonucleotide action); 2) favor cellular penetration of oligonucleotides (due to DNM); and 3) accumulate the conjugate in the nuclei, thus allowing the action of antigene oligonucleotides and DNM specifically on *MDR1* gene. The success of this approach at a cellular level opens the possibilities of further studies in vitro and in vivo.

Acknowledgments

We thank Lionel Dubost of the Mass Spectroscopy Service of the Muséum national d'Histoire naturelle for the mass spectral analysis.

References

Alahari SK, Dean NM, Fisher MH, Delong R, Manoharan M, Tivel KL, and Juliano RL (1996) Inhibition of expression of the multidrug resistance-associated P-glycoprotein of by phosphorothioate and 5′ cholesterol-conjugated phosphorothioate antisense oligonucleotides. *Mol Pharmacol* **50:**808–819.

Arimondo P, Bailly C, Boutorine A, Asseline U, Sun JS, Garestier T, and Helene C (2000) Linkage of a triple helix-forming oligonucleotide to amsacrine-4-carboxamide derivatives modulates the sequence-selectivity of topoisomerase II-mediated DNA cleavage. *Nucleosides Nucleotides Nucleic Acids* **19:**1205–1218.

Baldwin EL and Osheroff N (2005) Etoposide, topoisomerase II and cancer. *Curr Med Chem Anticancer Agents* **5:**363–372.

Bertram J, Palfner K, Killian M, Brysch W, Schlingensiepen KH, Hiddemann W, and Kneba M (1995) Reversal of multiple drug resistance in vitro by phosphorothioate oligonucleotides and ribozymes. *Anticancer Drugs* **6:**124–134.

Birg F, Praseuth D, Zérial A, Thuong NT, Asseline U, Le Doan T, and Hélène C (1990) Inhibition of simian virus 40 DNA replication in cv1 cells by an oligonucleotide covalently linked to an intercalating agent. *Nucleic Acids Res* **18:**2901–2907.

Brigui I, Djavanbakht-Samani T, Jolles B, Pigaglio S, and Laigle A (2003) Minimally modified phosphodiester antisense oligodeoxyribonucleotide directed against the multidrug resistance gene mdr1. *Biochem Pharmacol* **65:**747–754.

Buchini S and Leumann CJ (2003) Recent improvements in antigene technology. *Curr Opin Chem Biol* **7:**717–726.

Cantor CR, Warshaw MM, and Shapiro H (1970) Oligonucleotides interactions. III. Circular dichroism studies of the conformation of deoxyoligonucleotides. *Biopolymers* **9:**1059–1077.

Capobianco ML, De Champdore M, Arcamone F, Garbesi A, Guianvarc'h D, and PBA (2005) Improved synthesis of daunomycin conjugates with triplex-forming oligonucleotides. The polypurine tract of HIV-1 as a target. *Bioorg Med Chem* **13:**3209–3218.

Capobianco ML, De Champdore M, Francini L, Lena S, Garbesi A, and Arcamone F (2001) New TFO conjugates containing a carminomycinone-derived chromophore. *Bioconjug Chem* **12:**523–528.

Carbone GM, McGuffie E, Napoli S, Flanagan CE, Dembech C, Negri U, Arcamone F, Capobianco ML, and Catapano CV (2004) DNA binding and antigene activity of a daunomycin-conjugated triplex-forming oligonucleotide targeting the P2 promoter of the human c-myc gene. *Nucleic Acids Res* **32:**2396–2410.

Chen CJ, Clark D, Ueda K, Pastan I, Gottesman MM, and Roninson IB (1990) Genomic organization of the human multidrug resistance (MDR1) gene and origin of P-glycoproteins. *J Biol Chem* **265:**506–514.

Duan Z, Brakora KA, and Seiden MV (2004) Inhibition of ABCB1 (MDR1) and ABCB4 (MDR3) expression by small interfering RNA and reversal of paclitaxel resistance in human ovarian cancer cells. *Mol Cancer Ther* **3:**833–838.

Duca M, Oussedik K, Ceccaldi A, Halby L, Guianvarc'h D, Dauzonne D, Monneret C, Sun JS, and Arimondo PB (2005) Triple helix-forming oligonucleotides conjugated to new inhibitors of topoisomerase II: synthesis and binding properties. *Bioconjug Chem* **16:**873–884.

Fiallo M, Laigle A, Borrel MN, and Garnier-Suillerot A (1993) Accumulation of degradation products of doxorubicin and pirarubicin formed in cell culture medium within sensitive and resistant cells. *Biochem Pharmacol* **45:**659–665.

Frederick CA, Williams LD, Ughetto G, van der Marel GA, van Boom JH, Rich A, and Wang AH (1990) Structural comparison of anticancer drug-DNA complexes: adriamycin and daunomycin. *Biochemistry* **29:**2538–2549.

Garbesi A, Bonazzi S, Zanella S, Capobianco ML, Giannini G, and Arcamone F (1997) Synthesis and binding properties of conjugates between oligodeoxynucleotides and daunorubicin derivatives. *Nucleic Acids Res* **25:**2121–2128.

Gewirtz DA (1999) A critical evaluation of the mechanisms of action proposed for the antitumor effects of the anthracycline antibiotics adriamycin and daunorubicin. *Biochem Pharmacol* **57:**727–741.

Hande KR (2003) Topoisomerase II inhibitors. *Cancer Chemother Biol Response Modif* **21:**103–125.

Hu Q, Bally MB, and Madden TD (2002) Subcellular trafficking of antisense oligonucleotides and down-regulation of bcl-2 gene expression in human melanoma cells using a fusogenic liposome delivery system. *Nucleic Acids Res* **30:**3632–3641.

Hurley LH (2002) DNA and its associated processes as targets for cancer therapy. *Nat Rev Cancer* **2:**188–200.

Karukstis KK, Thompson EH, Whiles JA, and Rosenfeld RJ (1998) Deciphering the fluorescence signature of daunomycin and doxorubicin. *Biophys Chem* **73:**249–263.

Labroille G, Belloc F, Bilhou-Nabera C, Bonnefille S, Bascans E, Boisseau MR, Bernard P, and Lacombe F (1998) Cytometric study of intracellular P-gp expression and reversal of drug resistance. *Cytometry* **32:**86–94.

Laigle A, Fiallo MM, and Garnier-Suillerot A (1996) Spectral shape modifications of anthracyclines bound to cell nuclei: a microspectrofluorometric study. *Chem Biol Interact* **101:**49–58.

Liu C, Qureshi IA, Ding X, Shan Y, Huang Y, Xie Y, and Ji M (1996) Modulation of multidrug resistance gene (mdr-1) with antisense oligodeoxynucleotides. *Clin Sci* **91:**93–98.

Morassutti C, Scaggiante B, Xodo LE, Dapas B, Paroni G, Tolazzi G, and Quadrifoglio F (1999) Reduction of mdr1 gene amplification in human multidrug-resistant LoVo DX cell line is promoted by triple helix-forming oligonucleotides. *Antisense Nucleic Acid Drug Dev* **9:**261–270.

Napoli S, Negri U, Arcamone F, Capobianco ML, Carbone GM, and Catapano CV (2006) Growth inhibition and apoptosis induced by daunomycin-conjugated triplex-forming oligonucleotides targeting the c-myc gene in prostate cancer cells. *Nucleic Acids Res* **34:**734–744.

Nieth C, Priebsch A, Stege A and Lage H (2003) Modulation of the classical multidrug resistance (MDR) phenotype by RNA interference (RNAi). *FEBS Lett* **545:**144–150.

Pauly M, Kayser I, Schmitz M, Ries F, Hentges F, and Dicato M (1995) The human mdr1 (multidrug-resistance) gene harbours a long homopyrimidine.homopurine sequence next to a cluster of Alu repeated sequences in intron 14. *Gene* **153:**299–300.

Pérez-Tomás R (2006) Multidrug resistance: retrospect and prospects in anti-cancer drug treatment. *Curr Med Chem* **13:**1859–1876.

Quattrone A, Papucci L, Morganti M, Coronnello M, Mini E, Mazzei T, Colonna FP, Garbesi A, and Capaccioli S (1994) Inhibition of MDR1 gene expression by antimessenger oligonucleotides lowers multiple drug resistance. *Oncol Res* **6:**311–320.

Quigley GJ, Wang AH, Ughetto G, van der Marel G, van Boom JH, and Rich A (1980) Molecular structure of an anticancer drug-DNA complex: daunomycin plus d(CpG-pTpApCpG). *Proc Natl Acad Sci U S A* **77:**7204–7208.

Rutherford AV and Willingham MC (1993) Ultrastructural localization of daunomycin in multidrug-resistant cultured cells with modulation of the multidrug transporter. *J Histochem Cytochem* **41:**1573–1577.

Scaggiante B, Morassutti C, Tolazzi G, Michelutti A, Baccarani M, and Quadrifoglio F (1994) Effect of unmodified triple helix-forming oligodeoxyribonucleotide targeted to human multidrug-resistance gene mdr1 in MDR cancer cells. *FEBS Lett* **352:**380–384.

Stierlé V, Laigle A, and Jolles B (2004) The reduction of P-glycoprotein expression by small interfering RNAs is improved in exponentially growing cells. *Oligonucleotides* **14:**191–198.

Stierlé V, Laigle A, and Jolles B (2005) Modulation of MDR1 gene expression in multidrug resistant MCF7 cells by low concentrations of small interfering RNAs. *Biochem Pharmacol* **70:**1424–1430.

Sun BW, Babu BR, Sorensen MD, Zakrzewska K, Wengel J, and Sun JS (2004) Sequence and pH effects of LNA-containing triple helix-forming oligonucleotides: physical chemistry, biochemistry, and modeling studies. *Biochemistry* **43:**4160–4169.

Sun JS, François JC, Montenay-Garestier T, Saison-Behmoaras T, Roig V, Chassignol M, Thuong NT, and Hélène C (1989) Sequence-specific intercalating agents. Intercalation at specific sequences on duplex DNA via major-groove recognition by oligonucleotide intercalator conjugates. *Proc Natl Acad Sci U S A* **86:**9198–9202.

Sun JS, Giovannangeli C, Francois JC, Kurfurst R, Montenay-Garestier T, Asseline U, Saison-Behmoaras T, Thuong NT, and Helene C (1991) Triple-helix formation by alpha oligodeoxynucleotides and alpha oligodeoxynucleotide-intercalator conjugates. *Proc Natl Acad Sci U S A* **88:**6023–6027.

Sureau F, Chinsky L, Duquesne M, Laigle A, Turpin PY, Amirand C, Ballini JP, and Vigny P (1990) Microspectrofluorimetric study of the kinetics of cellular uptake and metabolization of benzo(a)pyrene in human T 47D mammary tumor cells: evidence for cytochrome P1450 induction. *Eur Biophys J* **18:**301–307.

Swift LP, Rephaeli A, Nudelman A, Phillips DR, and Cutts SM (2006) Doxorubicin-DNA adducts induce a non-topoisomerase II-mediated form of cell death. *Cancer Res* **66:**4863–4871.

Tonkinson JL and Stein CA (1994) Patterns of intracellular compartmentalization, trafficking and acidification of 5′-fluorescein labeled phosphodiester and phosphorothioate oligodeoxynucleotides in HL60 cells. *Nucleic Acids Res* **22:**4268–4275.

Wu H, Hait WN, and Yang JM (2003) Small interfering RNA-induced suppression of MDR1 (P-glycoprotein) restores sensitivity to multidrug-resistant cancer cells. *Cancer Res* **63:**1515–1519.

Address correspondence to: Dr. Paola B. Arimondo, Unité Mixte de Recherche 5153 Centre National de la Recherche Scientifique-MNHN USM0503, Institut National de la Santé et de la Recherche Médicale UR565, 43 rue Cuvier, 75005 Paris, France. E-mail: arimondo@mnhn.fr